Macromolecules

Article

pubs.acs.org/Macromolecules

Color-Tunable Amphiphilic Segmented π-Conjugated Polymer Nano-Assemblies and Their Bioimaging in Cancer Cells

Karnati Narasimha and Manickam Jayakannan*

Department of Chemistry, Indian Institute of Science Education and Research (IISER) Pune, Dr. Homi Bhabha Road, Pune 411008, Maharashtra India

Supporting Information

ABSTRACT: We report a unique color tunable amphiphilic segmented π-conjugated polymer design and their π-stack driven diverse self-assembled nanostructures and demonstrate their application as a new classes of aqueous luminescent nanoparticle probes for bioimaging in cervical and breast cancer cells. Oligo-phenylenevinylene (OPV) was employed as rigid luminescent π-core and oligo-ethyleneoxy chains were used as flexible spacers to construct new amphiphilic segmented π-conjugated polymers by Witting–Horner polymerization route. The rigidity of the π-core was varied using tricyclodecanemethyleneoxy, 2-ethylhexyloxy or methoxy pendants and appropriate π-core geometry was optimized to achieve maximum aromatic π-stacking interactions. Solvent-induced chain aggregation of the polymers exhibited a morphological transition from one-dimensional helical nanofibrous to three-dimensional spherical nanoassemblies in good/bad solvent combinations. This morphological transformation was accompanied by the fluorescence color change from blue-to-white-to-yellow. CIE color coordinates exhibited $x = 0.25$ and $y = 0.32$ for the white light followed by the collective emission from aggregated and isolated OPV chromophores. Electron and atomic microscopes, steady state photophysical studies, time-resolved fluorescent decay analysis, and dynamic light scattering method enabled us to establish the precise mechanism for the self-assembly of segmented OPV polymers. The polymers produced stable and luminescent aqueous nanoparticles of <200 nm diameter in water. Cytotoxicity studies in cervical and breast cancer cells revealed that these new aqueous luminescent polymer nanoparticles are highly biocompatible and nontoxic to cells up to 60 μg/mL. Cellular uptake studies by confocal microscope further exposed that these nanoparticles were internalized in the cancer cells and they were predominantly accumulated in the nucleus. The present investigation opens up new amphiphilic segmented π-conjugated polymer design for producing diverse supramolecular assemblies and also demonstrates their new application as biocompatible fluorescent nanoprobes for imaging in cancer cells.

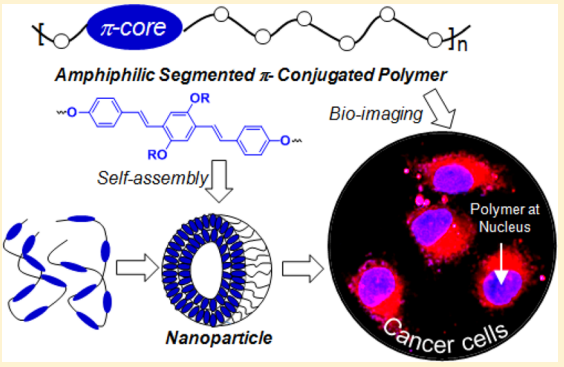

INTRODUCTION

Aqueous nanoassemblies of amphiphilic π-conjugated materials are emerging as important luminescent molecular probes for bioimaging[1,2] and sensing toxic metals[3−8] and as nanoscaffolds for delivery of genes[9] and drugs.[10−12] Amphiphilicity in π-conjugated aromatic polymers was typically introduced by anchoring flexible oligo- (or poly-) ethylene glycols as side chains in the π-conjugated backbones.[13] PEG-lated oligomers of thiophenes,[14−17] fluorenes,[18] phenylenes,[19−23] phenyleneethylenes,[24,25] phenylenevinylenes,[26,27] and perylenebisimides[28,29] were synthesized and self-assembled as vesicles, nanoparticles, and toroids[30,31] etc. Inspired by these self-assemblies of small molecular π-conjugates; recently, amphiphilic π-conjugated polymer based on rod−coil A−B−A triblock copolymer of oligo-phenylenevinylene (OPV) core and PEG corona were reported for nanofibrous and micellar assemblies.[32] Crown ether pendants were anchored on the poly(phenylenevinylene) backbone and the role of K^+ ion binding to produce nanoribbon morphology was studied.[33] The effect of potassium ion on the helical nanofiber morphology of A−B diblocks of poly(3-triethyelene glycol thiophene)-*block*-poly(3-hexylthiophene) was also reported.[34] Thermo and pH-responsive blocks of poly(3-hexylthiophene)-*block*-poly-(triethyeleneglycolallene)s was reported as white luminescent material.[35] In most of these examples; the self-assembly was primarily driven by the noncovalent interactions at the side chains and the π-conjugated polymer backbone was almost unaffected. Self-assembly of π-conjugated polymers that are responsive to change in the backbone is particularly important since it would provide new fundamental understanding of chain folding phenomena and also enabling the color-tuning via aromatic π−π stacking. Segmented π-conjugated polymers having rigid aromatic π-core and flexible alkyl or oligo ethyelene spacers in the backbone are unique classes of materials for the above purpose. In this design, the aromatic rigid core and flexible units can be selectively segregated in the

Received: March 31, 2016
Revised: May 12, 2016

DOI: 10.1021/acs.macromol.6b00660
Macromolecules XXXX, XXX, XXX−XXX

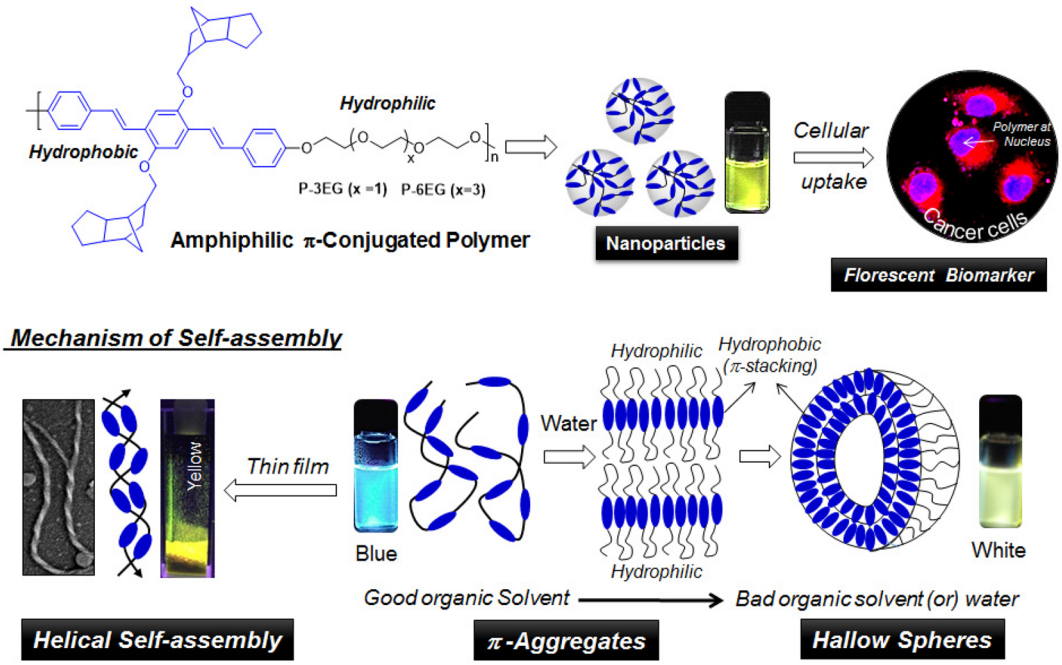

Figure 1. Segmented π-conjugated design for diverse polymer self-assembly and demonstrate their luminescent nanoassemblies as biomarkers in cancer cell imaging.

polymer matrix by weak noncovalent forces such as aromatic π-stacking and van der Waals forces. Karasz and co-workers reported segmented polymers of oligo-(1,4-phenyelenevinylene)s cores and demonstrated their application for blue light emitting diodes.[36] Pang and co-workers developed hybrid nanocomposites based on 1,3-meta-phenylene-bridged conjugated polymer and single-walled carbon nanotubes.[37,38] Segmented polymers with electron deficient and electron rich aromatic cores were self-assembled into helical amyliod-fibrils[39,40] and charger-transfer complexes.[41−43] Oligo-(1,4-phenylenevinylene)s segmented polymer and PCBM blends were prepared to study the photoinduced charge separation in solid state.[44] From our group, we reported segmented π-conjugated polymers based on carboxylic substituted 1,3-oligo-phenylenevinylenes as photosensitizer for Eu^{3+} ion[45] and their complexes were employed as triple detection probe for thermal, toxic metal ion and amino acids.[46] Further, oligo-1,4-phenyl-enevinylenes (OPV) segmented polymers were studied for helical donor−acceptor assemblies.[47] Semicrystalline OPV segmented polymers were designed and self-assembled as organogels to demonstrate their photonic $\lambda/4$ wave plates for optical switching applications.[48] These studies emphasized the importance of segmented π-conjugated polymers for photonic and electronic applications. Unfortunately, no effort has been taken until now to study the aqueous self-assembly of segmented π-conjugated polymers for biomedical applications. This is partially associated with the limited solubility of segmented π-conjugated polymers in water. The present investigation is aimed to address this problem by designing new classes of water-soluble amphiphilic π-conjugated OPV polymers and employ their aqueous stable nanoassemblies as nontoxic fluorescent biomarkers for cellular imaging in cancer cells. This new polymer design and imaging concept is shown in Figure 1.

The present investigation is emphasized to develop new classes of amphiphilic segmented π-conjugated polymers based on rigid and blue luminescent oligo-phenylenevinylene (OPV) π-core and variable oligo-ethyleneoxy flexible spacer. For this purpose, three OPV cores are chosen by varying the side chain anchoring groups as 2-ethylhexyloxy (EH, branched unit), tricyclodecanemethyleneoxy (TCD, rigid unit) and methoxy (Me) units. The selection of these pendants was done based on our recent efforts in resolving the crystal structures of OPVs to trace the role of substitution on the planarity of the molecules.[49−51] It was found that the substitution of TCD, EH, and Me in the vertical position and long tails in the longitudinal positions of OPV aromatic core produced planar geometry. Thus, these three planar OPV cores were chosen here to make new classes of segmented polymers to study their self-assembly. Thus, the combination of these OPV cores and ethylene glycol spacers provide an excellent opportunity to fine-tune the correct structural design to study the self-assembly process of segmented π-conjugated polymers. The photophysical studies revealed that emissions characteristics of the polymers were highly specific to their structure and the solvent compositions. The polymers underwent strong aromatic π-stacking and showed excellent color tunability from blue-to-white-to-yellow. This color tunability was accomplished by the morphological transition from nanofiber to spherical assemblies. The segmented polymers were found to produce stable aqueous luminescent nanoparticles. Cytotoxicity studies in cancer cells revealed that the polymer nanoparticles were nontoxic to cells and confocal microscopic analysis exhibited that the nanoparticles were readily taken by the cells and accumulated in the perinuclear environment. The overall investigation revealed that the new polymer design opens up a new opportunity to fine-tune their diverse nanoassemblies of segmented π-conjugated polymers and demonstrates their applications as fluorescent biomarker for the first time in cancer therapy.

EXPERIMENTAL SECTION

Materials. Hydroquinone, 4-hydroxybenzaldehyde, triethylene glycol, hexaethylene glycol, *p*-toluenesulfonyl chloride, triethylamine,

DOI: 10.1021/acs.macromol.6b00660
Macromolecules XXXX, XXX, XXX−XXX

triethyl phosphite, dimethyl sulfate, and potassium *tert*-butoxide (1 M in THF), were purchased from Aldrich Chemicals. HBr in glacial acetic acid, paraformaldehyde, K_2CO_3, and KOH were purchased locally. 1,8-Tricyclodecanemethanol was donated by Celanese Chemicals and Co. and has used without further purification. Solvents were purchased locally and purified by standard procedures. Tetraethyl ((2,5-dimethoxy-1,4-phenylene)bis(methylene))bis(phosphonate) (**3a**), tetraethyl ((2,5-bis((2-ethylhexyl)oxy)-1,4-phenylene)bis-(methylene))bis(phosphonate) (**3b**), and 1,4-bis-[(tricyclodecanemethyleneoxy)]-2,5-xylenediphosphonate (**3c**) were synthesized according to our earlier procedures.[48,49] Cervical cancer (HeLa) cells, breast cancer (MCF-7) cells were maintained in DMEM (phenol red containing, Gibco) containing 10% (v/v) fetal bovine serum (FBS) and 1% (v/v) penicillin−streptomycin at 37 °C under a 5% CO_2 atmosphere. For all the assays, cells were rinsed with 40% DPBS (Gibco), trypsinized using 0.05% trypsin (Gibco) and seeded in 96 well or 6 well (as per experiment) flat bottomed plastic plates (Costar). Fluoromount was obtained from Southern Biotech.

General Procedures. ^{1}H and ^{13}C NMR were recorded using 400 MHz JEOL NMR spectrometer. Infrared spectra were recorded using a Thermo-Scientific Nicolet 6700 FT-IR spectrometer in the solid state in KBr in the range of 4000−600 cm^{-1}. Mass analysis of precursors was determined by the Applied Biosystems 4800 PLUS MALDI TOF/TOF analyzer using TiO_2 as a matrix. The molecular weights of polymers were determined using gel permeation chromatography (GPC) which was performed by Viscotek triple detector setup and tetrahydrofuran as a solvent. TGA analysis was done using PerkinElmer STA 6000 simultaneous thermal analyzer. Differential scanning calorimetry (DSC) measurements had done by using TA Q20 DSC. The data were recorded at heating and cooling rate of 10 °C/min. The first heating cycle data was discarded since they possessed prehistory of the sample. Absorption spectra were recorded by using a PerkinElmer Lambda 45 UV spectrophotometer. Steady state emission and excitation spectra were recorded using Fluorolog-3 HORIBA JOBIN VYON fluorescence spectrophotometer. The quantum yields of the polymer aggregates were determined using quinine sulfate in 0.1 M H_2SO_4 (ϕ = 0.546) as standard. The solvent induced aggregation studies were performed using methanol (MeOH) and water as bad-solvents, respectively, for P-TCD-6EG by making different good-solvent/bad-solvent combinations. The stock solution was prepared by dissolving the polymer in THF, and chloroform and various combinations of THF/chloroform and methanol/water samples were prepared by maintaining the absorbance at ≈0.1. The time-resolved fluorescence lifetime measurements (TCSPC) were performed using a Fluorolog HORIBA JOBIN VYON fluorescence spectrophotometer. Fluorescence intensity decays were collected by a time-correlated single photon counting technique (TCSPC) setup from Horiba Jobin Yvon. 371 nm LED used for sample excitation. FE-SEM images were recorded using Zeiss Ultra Plus scanning electron microscope and the samples were prepared by drop casting on silicon wafers and coated with gold. Atomic force microscope images were recorded for drop-cast samples using Agilent instruments. The sample was drop casted on a freshly cleaved mica surface. The imaging was carried out in tapping mode using TAP-190AL-G50 probe from Budget sensors with a nominal spring constant of 48 N/m and the resonance frequency of 190. Dynamic light scattering (DLS) was performed using a Nano ZS-90 apparatus utilizing 633 nm red laser (at 90° angle) from Malvern Instruments. High Resolution-Transmission Electron Microscopy (HR-TEM) images were recorded using Technai-300 instrument by drop casting aqueous sample on Formvar-coated copper grids. LSM confocal microscope was used for cellular uptake images.

Synthesis of (Ethane-1,2-diylbis(oxy))bis(ethane-2,1-diyl) Bis(4-methylbenzenesulfonate) (1a). Triethylene glycol (5.0 g, 33.33 mmol) and *p*-toluenesulfonyl chloride (13.9 g, 73.33 mmol) were dissolved in dry DCM (50.0 mL). The solution was cooled (<5 °C), and powdered KOH (14.9 g, 266.00 mmol) was slowly added under nitrogen atmosphere. The reaction mixture was stirred for 4 h at 0 °C. Water (60.0 mL) was added and the product was extracted into DCM (100.0 mL). The organic layer was dried over anhydrous Na_2SO_4 and the solvent was removed to get product as white solid. The product was further purified by passing through silica gel column using ethyl acetate (30% v/v) in hexane as eluent. Yield = 13.7 g (90%). ^{1}H NMR (400 MHz, $CDCl_3$), δ ppm: 7.79 (d, 4H, Ar−**H**), 7.35 (d, 4H, Ar−**H**), 4.11 (t, 4H, Ar−$SO_2OCH_2CH_2$), 3.66 (t, 4H, Ar−$SO_2OCH_2CH_2$), 3.50 (s, 4H, Ar−$SO_2OCH_2CH_2$−OCH_2), and 2.45 (s, 6H, Ar−CH_3). ^{13}C NMR (100 MHz, $CDCl_3$), δ ppm: 144.86, 132.87, 129.8, 127.9, 70.65, 69.18, 68.71, and 21.63. FT-IR (cm-1): 2869, 1744, 1448, 1344, 1293, 1170, 1124, 1014, 978, 906, 849, 807, 772, 704, and 660. MALDI-TOF: calculated MW = 458.55; found m/z = 481.09 (M^++Na^+) and m/z = 497.43 (M^++K^+).

Synthesis of 3,6,9,12,15-Pentaoxaheptadecane-1,17-diyl Bis(4-methylbenzenesulfonate) (1b). Hexaethylene glycol (2.0 g, 7.10 mmol) was reacted with p-toluenesulfonyl chloride (3.0 g, 15.60 mmol) in the presence of KOH (3.2 g, 56.80 mmol) in dry DCM (30 mL) as described for **1a**. The product was further purified by column chromatography using ethyl acetate (60% v/v) in hexane as eluent. Yield = 3.14 g (75%). ^{1}H NMR (400 MHz, $CDCl_3$) δ ppm: 7.80 (d, 4H, Ar−**H**), 7.35 (d, 4H, Ar−**H**), 4.16 (t, 4H, Ar−$SO_2OCH_2CH_2$), 3.69 (t, 4H, Ar−$SO_2OCH_2CH_2$), 3.61−3.58 (m, 16H, Ar−$SO_2OCH_2CH_2$−OCH_2−), and 2.45 (s, 6H, Ar−CH_3). ^{13}C NMR (100 MHz, $CDCl_3$) δ ppm: 144.79, 132.82, 129.78, 127.90, 70.63, 70.49, 70.43, 70.39, 69.22, 68.58, and 21.59. FT-IR (cm^{-1}): 3394, 2878, 1719, 1646, 1600, 1453, 1351, 1294, 1215, 1171, 1097, 1031, 1005, 916, 813, 770, and 660. MALDI-TOF: calculated MW = 590.69; found m/z = 613.69 (M^+ + Na^+) and m/z = 641.02 (M^+ + K^+).

Synthesis of 4,4′-(((Ethane-1,2-diylbis(oxy))bis(ethane-2,1-diyl))bis(oxy))dibenzaldehyde (2a). 4-Hydroxybenzaldehyde (2.9 g, 24.0 mmol) and anhydrous K_2CO_3 (6.0 g, 44.0 mmol) were taken in dry acetonitrile (40.0 mL) and it was refluxed under nitrogen atmosphere. **1a** (5.0 g, 11.0 mmol) was added and the reaction was continued for 48 h at 80 °C under nitrogen atmosphere. The reaction mixture was poured into the water and then extracted with ethyl acetate. The organic layer was dried over anhydrous Na_2SO_4 and the solvent was evaporated to get product as white solid. It was further purified by column chromatography using 40% ethyl acetate/pet ether system. Yield = 2.7 g (69%). ^{1}H NMR (400 MHz, $CDCl_3$), δ ppm: 9.88 (s, 2H, Ar−C**H**O), 7.80 (d, 4H, Ar−**H**), 7.01 (d, 4H, Ar−**H**), 4.21 (t, 4H, Ar−OCH_2CH_2), 3.90 (t, 4H, Ar−OCH_2CH_2), and 3.77 (s, 4H, Ar−OCH_2CH_2−OCH_2). ^{13}C NMR (100 MHz, $CDCl_3$), δ ppm: 190.70, 163.78, 131.90, 130.11, 114.85, 71.93, 69.54, and 67.74. FT-IR (cm-1): 2887, 1687, 1600, 1598, 1571, 1506, 1457, 1425, 1392, 1352, 1303, 1249, 1213, 1147, 1099, 951, 916, 826, 791, and 647. MALDI-TOF: calculated MW = 358.39; found m/z = 381.10 (M^+ + Na^+) and m/z = 397.07 (M^+ + K^+).

Synthesis of 4,4′-((3,6,9,12,15-Pentaoxaheptadecane-1,17-diyl)bis(oxy))dibenzaldehyde (2b). 4-Hydroxybenzaldehyde (0.91 g, 7.4 mmol) was reacted with compound **1b** (2.00 g, 3.4 mmol) using anhydrous K_2CO_3 (1.87 g, 13.6 mmol) in dry acetonitrile (40 mL) as described for **3a**. It was further purified by column chromatography using ethyl acetate and pet ether mixture (1:1 v/v). Yield = 1.0 g (58%). ^{1}H NMR (400 MHz, $CDCl_3$), δ ppm: 9.88 (s, 2H, Ar−C**H**O), 7.82 (d, 4H, Ar−**H**), 7.02 (d, 4H, Ar−**H**), 4.21 (t, 4H, Ar−OCH_2CH_2), 3.88 (t, 4H, Ar−OCH_2CH_2), and 3.65−3.73 (m, 16H, Ar−OCH_2CH_2−OCH_2). ^{13}C NMR (100 MHz, $CDCl_3$), δ ppm: 191.00, 163.78, 132.92, 130.00, 114.82, 70.85, 70.57, 70.53, 69.41, and 67.70. FT-IR (cm-1): 2870, 2740, 1690, 1600, 1590, 1510, 1450, 1430, 1390, 1350, 1310, 1260, 1220, 1160, 1100, 1050, 951, 835, and 615. MALDI-TOF: calculated MW = 490.55; found m/z = 513.14 (M^+ + Na^+) and m/z = 529.10 (M^+ + K^+).

Synthesis of Segmented π-Conjugated OPV Polymers. Typical procedure is explained for P-TCD-3EG and other polymers were synthesized following similar procedure. Compound **3c** (0.5 g, 0.7 mmol) and compound **2a** (0.25 g, 0.7 mmol) were dissolved in dry THF (12 mL). The mixture was stirred under nitrogen atmosphere about 15 min at 25 °C. Potassium *tert*-butoxide (5 mL in 1 M THF) was added dropwise to the polymerization mixture under a nitrogen atmosphere and the stirring was continued at 25 °C for 24 h. The resultant yellow-green polymer solution was concentrated using rotavapor and it was poured into a large amount of methanol (50

DOI: 10.1021/acs.macromol.6b00660
Macromolecules XXXX, XXX, XXX−XXX

Scheme 1. Synthesis of the Main Chain Segmented Polymers Having Rigid OPV Core and Flexible Oligo-Ethyleneoxy Spacers

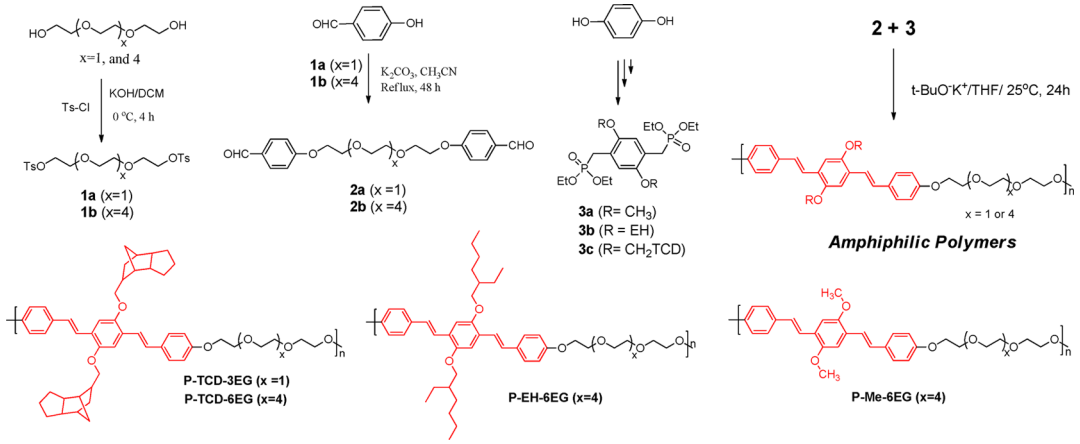

mL). The yellow-green polymer was filtered and washed with large amount of methanol. The polymer was redissolved in tetrahydrofuran, filtered and precipitated into methanol. The purification procedures were followed at least twice. Yield = 0.55 g (91%). ^{1}H NMR ($CDCl_3$, 400 MHz), δ ppm: 7.45 (d, 4H, **Ar**−**H**), 7.32 (d, 2H, J = 16 Hz, C**H**═C**H**), 7.13 (d, 2H, J = 20 Hz, C**H**═C**H**), 7.05 (s, 2H, **Ar**−**H**), 6.92 (d, 4H, **Ar**−**H**), 4.17 (t, 4H, OC**H**$_2$), 3.89 (t, 4H, OC**H**$_2$), 3.78 (d, 4H, OC**H**$_2$−TCD), and 2.5 to 1.50 (m, 30H, **aliphatic-H**). ^{13}C NMR ($CDCl_3$, 100 MHz), δ ppm: 158.27, 151.11, 131.11, 128.30, 127.58, 126.77, 121.80, 114.80, 111.04, 73.61, 70.89, 69.81, 67.46, 45.67, 45.27, 43.96, 41.27, 40.30, 34.74, 29.07, 27.98, 27.00, and 26.51. FT-IR (cm^{-1}): 2940, 2867, 1602, 1508, 1458, 1419, 1385, 1345, 1294, 1249, 1178, 1125, 1055, 1019, 967, 922, 848, and 818.

Synthesis of P-TCD-6EG. Compound **3c** (0.5 g, 0.7 mmol) was reacted with compound **2b** (0.343 g, 0.7 mmol) using potassium tert-butoxide (5 mL in 1 M THF) in dry THF (10 mL) described for **P-TCD-3EG** Yield = 0.61 g (87%). ^{1}H NMR ($CDCl_3$, 400 MHz) δ ppm: 7.44 (d, 4H, **Ar**−**H**), 7.31 (d, 2H, J = 16 Hz, C**H**═C**H**), 7.12 (d, 2H, J = 16 Hz, C**H**═C**H**), 7.04 (s, 2H, **Ar**−**H**), 6.91 (d, 4H, **Ar**−**H**), 4.16 (t, 4H, OC**H**$_2$), 3.87 (t, 4H, OC**H**$_2$), 3.74 (m, 16H, OC**H**$_2$), 3.72 (d, 4H, OC**H**$_2$−TCD), and 2.5 to 1.50 (m, 30H, **aliphatic-H**). ^{13}C NMR ($CDCl_3$, 100 MHz) δ ppm: 158.25, 151.08, 131.06, 128.30, 127.55, 126.63, 121.72, 114.78, 111.0, 73.60, 70.76, 70.55, 69.70, 67.43, 45.64, 45.24, 43.95, 41.26, 40.27, 34.73, 29.05, 28.0, 27.0, and 26.51. FT-IR (cm^{-1}): 2936, 2864, 1647, 1600, 1506, 1457, 1417, 1382, 1349, 1292, 1241, 1178, 1102, 1019, 959, 844, and 814.

Synthesis of P-Me-6EG. Compound **3a** (0.5 g, 1.1 mmol) was reacted with compound **2b** (0.343 g, 1.1 mmol) using potassium *tert*-butoxide (6 mL in 1 M THF) in dry THF (10 mL) as described for **P-TCD-3EG.** Yield = 0.48 g (77%). ^{1}H NMR ($CDCl_3$, 400 MHz), δ ppm: 7.47 (d, 4H, **Ar**−**H**), 7.34 (d, 2H, J = 16 Hz, C**H**═C**H**), 7.10 (s, 2H, **Ar**−**H**), 7.05 (d, 2H, J = 16 Hz, C**H**═C**H**), 6.90 (d, 4H, **Ar**−**H**), 4.14 (t, 4H, OC**H**$_2$), 3.90 (s, 6H, OC**H**$_3$), 3.86 (t, 4H, OC**H**$_2$), and 3.73−3.67 (m, 16H, OC**H**$_2$). ^{13}C NMR ($CDCl_3$, 100 MHz), δ ppm: 158.34, 151.29, 130.82, 128.23, 127.70, 126.44, 121.14, 114.74, 108.84, 70.78, 70.58, 70.54, 69.69, 67.41, and 56.31. FT-IR (cm^{-1}): 2969, 1688, 1598, 1503, 1456, 1404, 1348, 1293, 1239, 1209, 1098, 1033, 953, and 810.

Synthesis of P-EH-6EG. Compound **3b** (0.5 g, 0.8 mmol) was reacted with compound **2b** (0.386 g, 0.7 mmol) using potassium tert-butoxide (5 mL in 1 M THF) in dry THF (10 mL) as described for **P-TCD-3EG.** Yield = 0.58 g (90%). ^{1}H NMR ($CDCl_3$, 400 MHz), δ ppm: 7.45 (d, 4H, **Ar**−**H**), 7.35 (d, 2H, J = 16 Hz, C**H**═C**H**), 7.08 (d, 2H, J = 16 Hz, C**H**═C**H**), 7.10 (d, 2H, **Ar**−**H**), 6.91 (d, 4H, **Ar**−**H**), 4.15 (t, 4H, OC**H**$_2$), 3.87 (t, 4H, OC**H**$_2$), 3.67 (m, 16H, OC**H**$_2$), 3.94 (d, 4H, OC**H**$_2$−EH), 2.02 (m, 4H, OCH2-C**H**$_2$−C**H**$_2$), 1.82 (m, 2H, OCH$_2$−C**H**−CH$_2$), 1.64−1.38 (m, 18H, **aliphatic-H**), 0.98 (t, 6H, C**H**$_3$), and 0.92 (t, 6H, C**H**$_3$). ^{13}C NMR ($CDCl_3$, 100 MHz), δ ppm: 158.29, 151.00, 131.04, 128.00, 127.56, 126.69, 121.50, 114.79, 111.08, 71.76, 70.82, 70.61, 70.57, 69.72, 67.45, 39.76, 30.92, 29.25, 23.10, 14.12, and 11.31. FT-IR (cm^{-1}): 2922, 2866, 1682, 1602, 1508, 1460, 1419, 1383, 1348, 1292, 1243, 1200, 1106, 1032, 959, 847, 818, 729, and 643.

Aqueous Self-Assembly of P-TCD-6EG Polymer. In a typical experiment, 2.0 mg of the polymer was dissolved in DMSO (1.5 mL) and THF (0.5 mL). Deionized water (3.0 mL) was added dropwise into the polymer solution. The resulting solution was stirred at 25 °C under dark conditions for 4 h. The solution was transferred to the semipermeable membrane having MWCO 2000 and then dialyzed against a large amount of deionized water for 48 h. Fresh water was replenished periodically to ensure the removal of THF and DMSO from the dialysis membrane. The dialyzed solution was filtered, lyophilized, and stored at 4 °C for further usage.

Cell-Viability Assay. The tetrazolium salt, 3-(4,5-dimethylthiazol-2-yl)-2,5-diphenyltetrazolium bromide (MTT) assay was employed in order to study the cytotoxic effect of the P-TCD-6EG polymer nanoparticles in HeLa and MCF7 cells. For this experiment, a 96-well plate (Corning, USA) was used and each of its wells were seeded with 1000 cells in 100 μL of DMEM with 10% FBS (fetal bovine serum) and these were allowed to adhere for 16 h. The media from each well was aspirated followed by addition of various concentrations of the polymer to each well. These were added in triplicates corresponding to individual experiments. Cells in DMEM with FBS in the absence of polymer were also maintained in triplicates as a blank control. The 96 well plate was incubated for 72 h without changing the media. After 72 h medium from each well was aspirated and 100 μL of MTT solution (a freshly prepared stock of MTT in sterile PBS (5 mg/mL) diluted to 50 μg/mL in DMEM) was added. These were allowed to incubate for another 4 h at 37 °C. The formation of purple formazan crystals was observed that developed due to the reduction of MTT by mitochondrial dehydrogenase enzyme from viable cells, and the media from each well was aspirated and 100 μL of DMSO was added to the resultant crystals giving purple solutions in each well. The absorbance from formazan crystals was immediately recorded using microplate reader at 570 nm (Varioskan Flash), which gave a representative of the number of viable cells per well. Values corresponding to each triplicate (of control and polymer treated cells) were determined and their mean was used for calculations. In the triplicates, any value that deviated from rest two were discarded. The mean of blank control set as 100% (corresponding to viable cells) and relative percentage values for polymer nanoparticle were calculated with respect to this.

Cellular Uptake Studies. Flame-dried coverslips were taken in 6 well plate in DMEM medium containing 10% FBS. On the surface of these coverslips, cells were seeded at a density of 1 × 10^5 cells and these were incubated at 37 °C for 16 h. The cells in each well, thus grown, were treated with required concentrations of P-TCD-6EG polymer nanoparticles. This was incubated at 37 °C for 4 h under CO_2 environment and then the media was aspirated from each well, and the cells were washed twice with PBS (2 × 1 mL) and fixed with 4%

DOI: 10.1021/acs.macromol.6b00660
Macromolecules XXXX, XXX, XXX−XXX

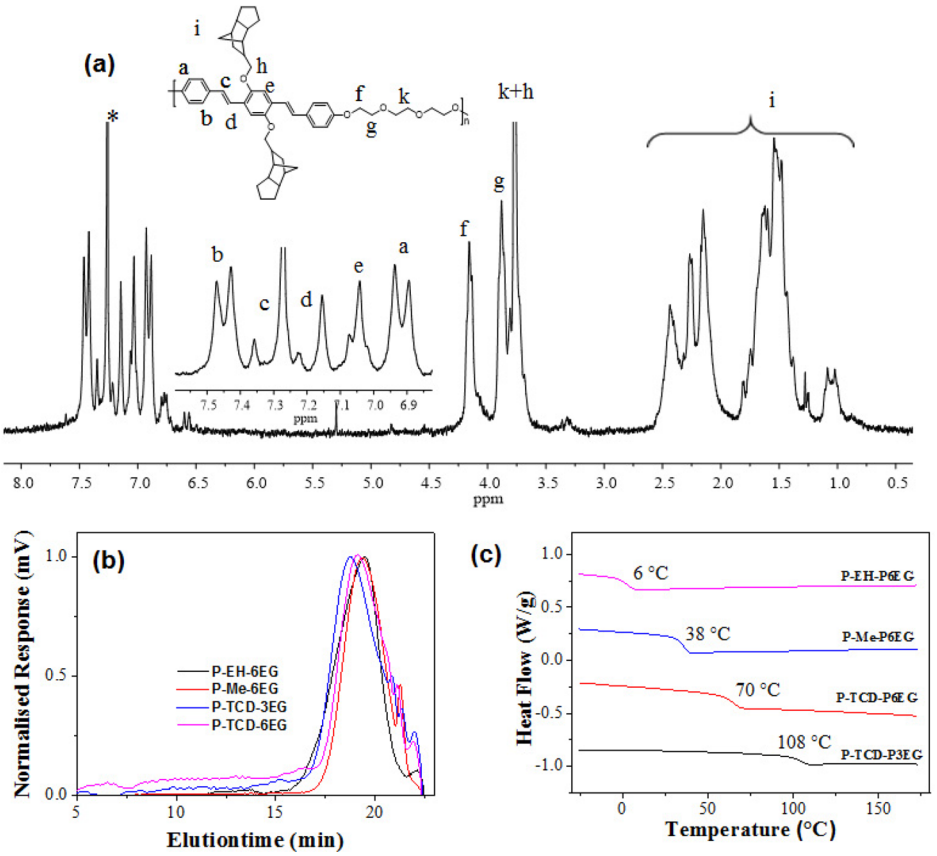

Figure 2. ^{1}H NMR spectrum of P-TCD-3EG in $CDCl_3$ (a). GPC chromatograms of the segmented polymers in THF (b). DSC thermograms of polymers in heating cycles at 10 °C/min (c).

paraformaldehyde solution in PBS for 10 min at room temperature. The cells were washed twice with PBS (2 × 1 mL) and stained with phalloidin (red) conjugated to Alexa 610 (Invitrogen) diluted 1:100 in 5% BSA solution in PBS. These were incubated for 2 min, at room temperature under dark conditions, and then the excess dye was washed from the plate and the cells were gently rinsed with PBS. The coverslips were mounted on slides using Fluoromount mounting medium (Southern Biotech) and were left for drying overnight at room temperature in the dark. The cells were imaged using a confocal microscope using the λ 405 nm (blue channel) and λ 560 nm (red channel) lasers. Images thus obtained were analyzed using ImageJ analysis software, and the image for each channel was separated and merged.

RESULTS AND DISCUSSION

Synthesis and Characterization of Segmented Polymers. New classes of segmented polymers were synthesized through multistep reactions as shown in Scheme 1. ω-Bis-benzaldehydes (compounds **2a**−**2b**) were synthesized by reacting 4-hydroxybenzaldehyde with appropriate tosylates of oligo-ethylene glycols (compounds **1a**−**1b**). Three bisphosphonate esters having variable aliphatic and cycloaliphatic substitutions such as methoxy (**3a**), 2-ethylhexyloxy (**3b**), and tricyclodecanemethyleneoxy (**3c**), were synthesized following our earlier procedure.[48,49] The polymerization of monomers **3a**−**3c** with equimolar amounts of bis-benzaldehydes (**2a**−**2b**) under Wittig−Horner conditions produced respective segmented polymers consisting of rigid oligo-phenylenevinylenes and oligo-ethyleneoxy flexible spacers in the polymer backbone. These polymers were referred as **P-Y-X**, where Y represents Me, EH or TCD for the methoxy, ethylhexyloxy, or tricyclodecanemethyleneoxy units, respectively, and X stands for a number of oligoether units present in the flexible alkyl chains such as triethylene glycol (3EG) and hexaethylene glycol (6EG), respectively. For example, the TCD polymer with 6-EG unit is referred as P-TCD-6EG. The chemical structures of all the polymers are shown in Scheme 1.

The structures of the polymers were characterized by ^{1}H NMR, ^{13}C NMR, and FT-IR. ^{1}H NMR spectra of the P-TCD-3EG polymer are shown in Figure 2a, and different types of protons in the chemical structure are assigned alphabetically (see Figure S1 for NMR spectra of other polymers). The ^{1}H NMR spectrum of the P-TCD-3EG polymer showed peaks from 7.46 to 6.90 ppm with an appropriate splitting pattern corresponding to aromatic phenylenevinylene protons (see Figure 2a). The two doublets which belong to trans-vinylene protons (c and d protons) appeared at 7.36 and 7.09 ppm (coupling constant J = 16 Hz). The peaks appeared at 7.43, 7.11, and 6.90 ppm were assigned to protons b, e, and a, respectively. The broad triplets at 4.10 ppm, 3.86 ppm were attributed to Ar−O**C**H_2**C**H_2 and 3.78 ppm is belonging to Ar−O**C**H_2−TCD protons, respectively. Among the two doublets in the vinyl protons, one of them merged with solvent peak at 7.26 ppm (see Figure 2a). TCD protons appeared below 3.5 ppm. Similarly, ^{13}C NMR spectra of the polymer P-TCD-3EG showed the peaks for expected structure formation (see Figure S2). The molecular weights of the polymers were determined by gel permeation chromatography (GPC) in tetrahydrofuran using polystyrene standards. The GPC chromatograms of the polymers appeared as monomodal distribution except for P-TCD-3EG which showed was partially soluble in THF (see

DOI: 10.1021/acs.macromol.6b00660
Macromolecules XXXX, XXX, XXX−XXX

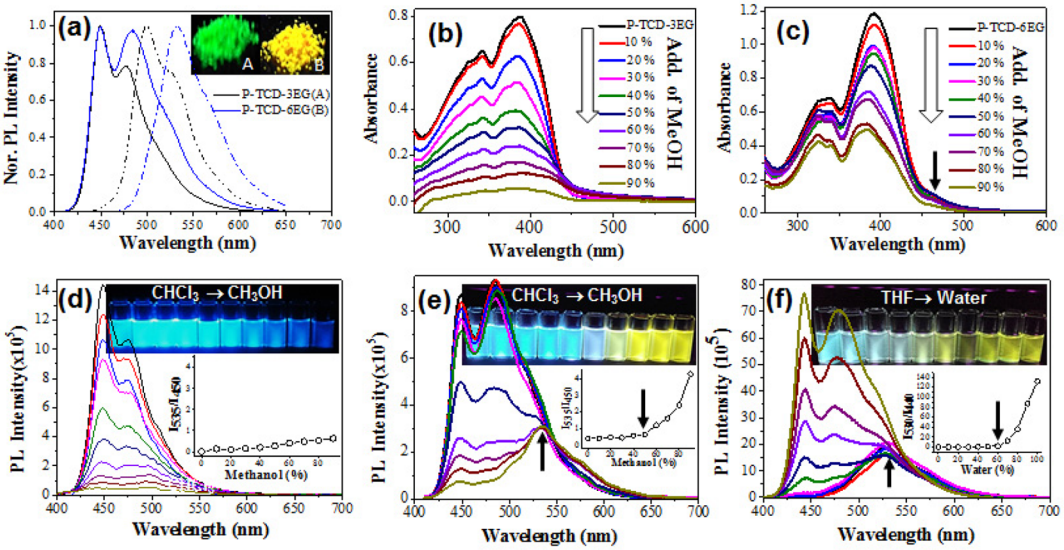

Figure 3. Emission spectra of P-TCD-3EG and P-TCD-6EG in $CHCl_3$ (solid line) and thin film (dotted line) and the photographs are taken for the powder sample on quartz plate upon photoexcitation (a). Absorbance spectra of P-TCD-3EG (b) and P-TCD-6EG (c) in methanol/chloroform mixture. Emission spectra of P-TCD-3EG (d) and P-TCD-6EG (e) in methanol/chloroform mixture. Emission spectra of P-TCD-6EG (f) in water/tetrahydrofuran solution. The photographs are taken for polymer solutions in vials upon photoexcitation by UV-light at 365 nm. The concentration of the polymers were maintained as 2.5×10^{-5} M.

Figure 2b). The molecular weights of the polymers were obtained as M_w = 16 800 to 28 000 g/mol with a polydispersity of 2.0 to 3.5 (see Table ST1). The Witting−Horner polymerization route is typically known to produce polymers with 10−15 repeating units as observed by us[51,47] and others.[36] For biomedical applications, polymer molecular weights of <40 000 g/mol are preferred due to their easy clearance through the kidney. Hence, the custom designed polymers have molecular weight <28 000 g/mol which is less than the acceptable range for biomedical imaging applications.

Thermogravimetric analysis (TGA) of the polymers showed that the polymers were thermally stable up to 350 °C (see Figure S3). Differential scanning calorimetry (DSC) analysis of polymers was carried out at the heating/cooling cycle rate of 10 °C/min. DSC thermograms of the polymers at 10 °C/min heating are shown in Figure 2c. All the polymers were found to be completely amorphous and the DSC thermograms have shown only glass transition temperature (T_g) in cooling and heating cycles (see Figure S4 for their cooling cycles). The T_g's of the polymers gradually decreased from 108 to 70 °C upon increasing the length of the oligoethylene glycol segment from 3EG to 6EG in P-TCD-3EG to P-TCD-6EG. This trend is attributed to the increase in the flexibility of the polymer chains with an increase in the number of oligo-ethyleneoxy units in the segmented polymer chain. Further, the comparison among the 6EG spacer polymers revealed that the T_g values decreased with a decrease in the rigidity of the polymers in the following order TCD > Me > EH from 70 to 6 °C. This observation indicates that the cycloaliphatic TCD units introduced much higher rigidity in the OPV core compared to other two side chains. The variation of T_g values from 108 to 6 °C in the segmented polymers are clear indication that the rigidity of the π-conjugated units and varying the EG-spacers in the backbone are crucial factor for the rigidity of the structure. Among all these polymers, TCD units appeared to be very unique in producing highly rigid polymers with higher T_g values.

Aromatic π-Stack Aggregation and Emission Color-Tuning. The segmented OPV polymers are designed with different substitution in the central aromatic ring and flexible oligoethyelneoxy chains. This arrangement facilitates the strong aromatic π-stacking interaction among the OPV chromophores to maximize the self-assembly process. To study this effect in solution and solid state (in a thin film); the polymer samples were subjected to steady state photophysical studies and time-resolved fluorescent decay properties. The absorbance and emission spectra of P-TCD-3EG and P-TCD-6EG polymers were found to be almost identical in solution (see Figure 3a). In the solid state, the emission spectra of the hexaethylene glycol segmented P-TCD-6EG polymer showed 50 nm red-shift compared to the P-TCD-3EG polymer (see absorbance spectra in Figures S5 and S6). This suggests that the TCD-substituted OPV chromophores became more facile to undergo self-assembly via aromatic π-interaction when they were separated by longer segmented spacers. The photographs of these polymer samples in Figure 3a showed greenish and yellow emission for P-TCD-3EG and P-TCD-6EG with respect to the 50 nm shift in their emission wavelength. This suggests that the increasing oligoethyleneoxy segments between the adjacent OPVs increased the π-stacking interaction among the chromophores. The strong π−π stacking among the OPV cores induced emission-shift. This trend is attributed to the increasing the OPV self-aggregation with an increase in the segmented spacer length. Unlike P-TCD-6EG, the other 6EG-spacer polymers P-EH-6EG and P-ME-6EG did not show any significant color change in their emission spectra (see Figure S6). Thus, the aromatic π-stacking interaction in the segmented polymer was mainly driven by the types of the OPV chromophores and in the present case TCD-OPV was very unique in exhibiting maximum packing among the various OPV π-cores. The segmented polymer with hexaethylene glycol (6EG) was found to be more flexible than triethylene glycol spacer (3EG) which was evident from their T_g values (see Figure 2c). The highly flexible chains possess high degree of

DOI: 10.1021/acs.macromol.6b00660
Macromolecules XXXX, XXX, XXX−XXX

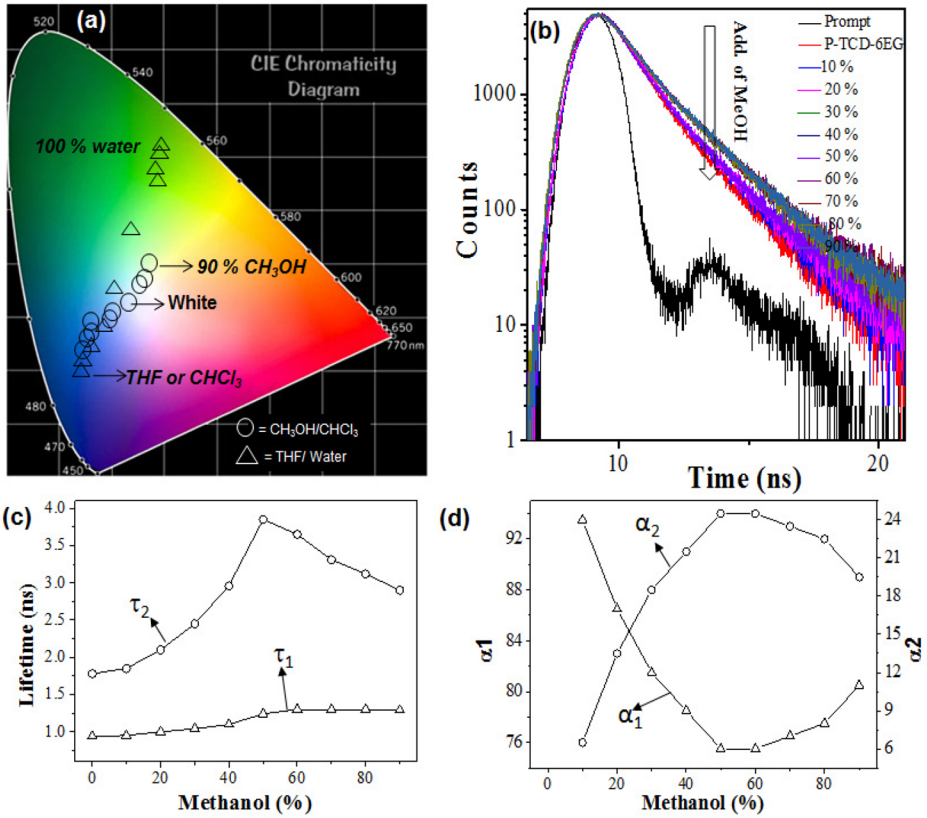

Figure 4. CIE color coordinates of P-TCD-6EG polymer solution in THF + water (Δ) and $CHCl_3$ + methanol (O) (a). TCSPC decay profiles of P-TCD-6EG polymers in methanol+chloroform solvent mixtures (b). Plots of fluorescent lifetime τ_1 and τ_2 (c) and fractional contribution α_1 and α_2 (d) of the polymers in methanol + chloroform solvent mixtures. The concentrations of the polymers were maintained as 2.5×10^{-5} M.

freedom for both intrachain and interchain folding; as a result, the OPV could undergo strong aromatic π-stacking interactions. On the other hand, the shorter spacers (3EG) did not have sufficient flexibility to bend the chains which restrict the overlap between the OPV chromophores. These studies suggested that the longer segmented OPV polymers (>6 EG units) have high tendency to undergo self-organization via aromatic π-stacking interaction. On the other hand, the shorter segmented lengths (<3 EG units) did not provide enough flexibility for TCD-OPV chromophores in the polymer backbone for π-stacking induced self-assembly.

Typically polymer chains are expected to adopt either expanded or coil-like conformation with respect to the solvents in which they are present. For instance, a good solvent maximizes the solvent−polymer interaction and solvates the polymer chains in the expanded chain conformation whereas in poor solvents the polymer chains predominately adopt coil-like conformation and precipitate the polymers.[47,50] Therefore, by appropriately choosing the combination of good and poor solvents; one can easily control the expanded or coil-like conformation in polymer chains. Since the segmented polymers showed very good spacer dependent self-assembly in the solid state, their solvent induced aggregated self-assembly were studied to trace their chain folding phenomena. For this purpose, two solvent combinations are chosen: (i) methanol/chloroform and tetrahydrofuran/water. Absorbance spectra of polymers (see Figure 3, parts b and c) showed a decrease in absorbance with an increase in methanol content in the solvent mixture. This trend is attributed to the variation in the molar extinction coefficient of OPV chromophores in the solvent combination.[51] Interestingly P-TCD-6EG polymer showed an additional peak at 470 nm (shown by the arrow) with respect to the formation of π-induced OPV aggregates. This trend clearly indicates that P-TCD-6EG polymers have a high tendency for π-induced aggregation upon increasing the amount of methanol in the polymer solution. The emission spectra of P-TCD-3EG and P-TCD-6EG polymers in methanol/chloroform solvent combinations are shown in Figure 3, parts d and e, respectively (see Figure S7 for P-EH-6EG and P-Me-6EG). The drastic decrease in the emission intensity of the spectra was attributed to the reduction in their molar extinction coefficient in their absorbance spectra. Interestingly, the long segmented P-PCD-6EG polymer showed excellent color tuning ability with the formation of new emission peak at higher wavelength region (which was absent in their lower counterpart P-TCD-3EG, see Figure 3d). The emission peak at λ_{em} = 450 nm was assigned to isolated OPV chromophores and the new peak at λ_{em} = 535 nm was assigned to OPV chromophore in the aggregated state (shown by the arrow). The comparison of the solid state emission maxima of P-TCD-6EG at 535 nm (see Figure 3a) and solvent induced aggregated emission peak at 537 nm (see Figure 3e) revealed that the OPV chromophores had attained maximum aromatic π-staking in methanol + chloroform mixture as equivalent to that of their interaction in the solid state. Further, to quantify the extent of aggregation in P-TCD-6EG (also P-TCD-3EG), the ratio of the peaks λ_{em} = 535/450 nm were plotted against the solvent composition and shown as an inset in Figures 3d and 3e. These plots showed distinct break points at 40−50% methanol in chloroform for long segmented polymer for P-

DOI: 10.1021/acs.macromol.6b00660
Macromolecules XXXX, XXX, XXX−XXX

TCD-6EG (see Figure 3e) whereas the change is insignificant in short segmented polymer P-TCD-3EG (see Figure 3d). Additionally, the polymer solution of P-TCD-6EG showed excellent color tuning from blue-to-white-to-yellowish with an increase in the methanol composition in the solvent mixture (see the photographs in Figure 3e). Similar solvent induced aggregation experiments were carried out for P-EH-6EG and P-Me-6EG and these studies indicated that these polymers did not show π-stacking interaction unlike P-TCD-6EG (see Figure S7). Based on these studies, it can be concluded that the TCD-OPV chromophores exhibited excellent π-induced aggregation compared to ethylhexyloxy and methoxy units in the segmented polymers. Furthermore, it is rather clear that the placing of the π-conjugated chromophores apart in the segmented backbone maximize the π-stack induced aggregation in segmented π-conjugated polymers.

In order to study the aqueous self-assembly of π-induced aggregation, the P-TCD-x polymers were dialyzed against large amount of water using cellulose semipermeable membrane of MWCO of 2000 g/mol for 48 h. The reservoir was continuously replenished with fresh water to ensure the removal of DMSO and THF from the polymer solution. Among the two segmented polymers, only P-TCD-6EG was found to produce a stable aqueous solution whereas P-TCD-3EG (also P-Me-6EG) precipitated from water and was not stable during the dialysis in water. The optical density of P-TCD-6EG was chosen as 0.1 and the composition of the solutions were varied from 10 to 90 v/v of THF + water. The emission spectra of the P-TCD-6EG (see Figure 3f) showed the decrease in the emission intensity of the isolated OPV chromophores (at λ_{em} = 450 nm) and new emission peak appeared for aggregated OPV chromophores (at λ_{em} = 535 nm). The comparison of emission characteristics in water + THF combinations (see Figure 3f) with its solid state emission spectra of P-TCD-6EG (see Figure 3a) [or its aggregation in $CHCl_3$ + methanol in Figure 3e] revealed that TCD-OPV chromophores attained maximum aromatic π-stacking in >50% water in THF or in 100% water. Further, to quantify the extent of aggregation in P-TCD-6EG, the ratio of the peaks λ_{em} = 535/450 nm were plotted against the water/THF composition and shown as an inset in Figure 3f. This plot showed a distinct break point at 40−50% of THF in water for P-TCD-6EG. The polymer P-TCD-6EG showed excellent color tuning from blue to white to yellowish with an increase in the water content in the solution (see Figure 3f) or in water. The emission spectra of P-TCD-6EG in the solvent combinations were fed into CIE color coordinate diagram and the details are shown in Figure 4a. It is very interesting to notice that the P-TCD-6EG chains could be transforming its emission color from blue-to-white-to-yellow. At the intermediate solvent combination (50:50%), both expanded and coil-like conformation coexisted in the polymer solution to produce white emission. This was further supported by the break points seen in the inset in Figure 3, parts e and f. White light emission in the present system is observed due to the merging of blue and greenish yellow emission of isolated and aggregated OPV chromophores, respectively. The CIE color coordinates for the white emission was obtained as x = 0.25 and y = 0.32 which is in accordance for white emission as reported by us and others.[53,54,35] On the other hand, other polymers P-TCD-3EG, P-Me-6EG, and P-EH-6EG did not show such variation in the emission colors in the CIE color coordinates (see Figure S8). The segmented polymers with P-Me-6EG polymers did not show the color tuning unlike the P-TCD-6EG polymers (both polymer have same spacer length; however, their substitution in the OPV cores varied). The difference for these behaviors can be correlated based on their structural arrangements from the single crystal data of methoxy substituted OPVs.[49] The three aryl rings in the methoxy substituted OPVs do not occupy the same plane and they were tilted at either side by more than 34.02°. As a result, the OPVs became nonplanar and expected to have less probability for the aromatic π-stacking for color tune-ability. On the other hand, the π-core consisting of the aryl rings in TCD substituted OPVs showed planar geometry in the single crystal structure.[50] Thus, strong aromatic π-stacking interactions were feasible among the TCD-OPVs for their unique color tuning-ability in the present segmented polymer system. This observation clearly supports that the P-TCD-6EG segmented polymer is very unique in structural design to undergo aromatic π-stacking to produce diverse luminescent colors. It is important to note that the present segmented OPV polymer design is one of the first examples to report color tuning in single π-conjugated polymer system. The fluorescence quantum yields for the polymer solutions were determined using quinine sulfate as standard.[47,51] The quantum yields are plotted for both chloroform+methanol and THF+water solvent combinations (see Figure S9). The quantum yields were found to decrease with the increase in the poor solvent amount (methanol or water) in the polymer solutions. The decrease in the quantum yield is attributed to the aggregated induced fluorescence quenching of the π-conjugated OPV chromophores.[52]

Time correlated single photon counting (TCSPC) was employed to study the excited state luminescent life times of P-TCD-6EG polymer in methanol/chloroform solvent combinations. The OPV chromophore was excited with 371 nm Nano LED source and the TCSPC decay profiles of the polymer are shown in Figure 4b. The decay profiles of the polymer did not show many changes; however, a small decrease in the decay with an increase in the methanol compositions could be observed (see Figure 4b). These luminescence decay profiles were fitted with biexponential decay and their lifetime values are given in Table ST-2 in the Supporting Information. The τ_1 and τ_2 values and their fractional contributions are plotted and shown in Figure 4, parts c and d. τ_1 and τ_2 represent the decay rate constant for isolated and aggregated OPV chromophores, respectively. On increasing the methanol concentration, the value of τ_2 increased up to 60% MeOH/$CHCl_3$ and then attained a plateau. The higher τ_2 values indicate that the aggregated species indeed can fluorescence for a longer period. The fractional contributions were also showed break-points at 40−50% methanol in the solvent mixtures. Hence, it may be concluded that the TCSPC decay studies supported the color tuning ability of the P-6EG polymer with a high luminescent lifetime in all three colors blue, white and yellow. On the basis of the photophysical studies, it may be concluded that the segmented OPV polymer possessed unique polymer geometry to undergo chain folding by the strong aromatic π-stacking on the backbone of the polymer chains.

Nanofibers, Hollow Spheres, and Nanoparticles. It is very clear from the photophysical studies that the P-TCD-6EG chains are capable of undergoing π-induced aggregation for color tuning from blue-to-white-to-yellow. To visualize the size and shape of the polymer aggregates accompanied by the above transition, the P-TCD-6EG samples in $CHCl_3$ + methanol solvent combinations were subjected to FE-SEM and AFM

DOI: 10.1021/acs.macromol.6b00660
Macromolecules XXXX, XXX, XXX−XXX

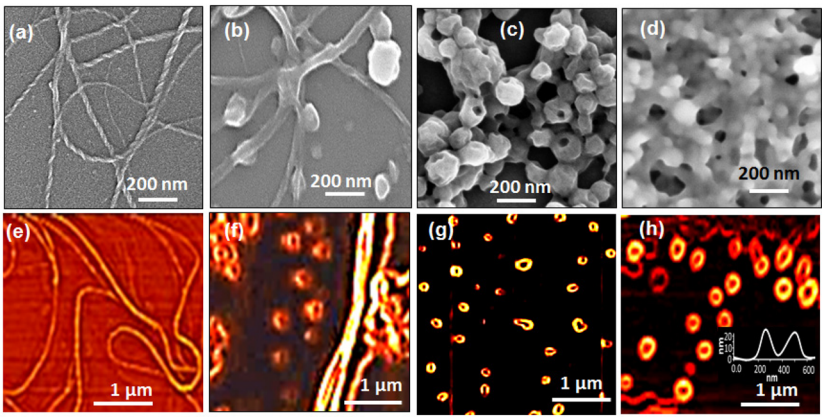

Figure 5. FE-SEM images of P-TCD-6EG polymer in chloroform (a) and 20% (b), 40% (c), and 60% (d) of methanol in chloroform. AFM images of P-TCD-6EG polymer in chloroform (e) and 20% (f), 40% (g), and 60% (h) of methanol in chloroform/methanol. The concentrations of the polymers were maintained as 1×10^{-5} M.

analysis. These morphological features are given in Figure 5. The polymer showed nanofibrous morphology in chloroform alone (see Figure 5a) and the length of helical nanofibers was estimated to be 10 to 20 μm and their widths were determined to be 20−50 nm in diameter. The closer observation revealed that thin and highly helical nanofibers were produced by the longer segmented P-TCD-6EG. HR-TEM image was also further confirmed the existence of nanofibrous morphology in P-TCD-6EG (see Figure S10). The P-TCD-6EG chains showed an excellent morphological transition from nanofibers to spherical nanoassemblies upon increasing the methanol amount in the solvent mixture (see Figure 5b−d). The closer observation of spherical assemblies in Figure 5c revealed that they are hollow. The observation was attributed to the folding or collapsing of the nanofibers into hollow spheres. At higher methanol content, the morphology was turned completely into a spherical particle in nature (see Figure 5d).

Atomic force microscope (AFM) images of P-TCD-6EG in chloroform showed highly twisted helical nanofibrous (see Figure 5e) as seen in their FE-SEM images. AFM analysis showed the length of the fibers 5 to 10 μm with a thickness of 60 nm. AFM images of the polymer samples in solvent mixtures were recorded and shown in Figure 5f−h. At 20% methanol compositions, the polymer exhibited both helical nanofibers and hollow spheres (see Figure 5f). Upon increasing the methanol amount, the formation of hollow spheres became predominant and the nanofibrous morphology vanished completely (see Figure 5, parts f and h). At 40−60% methanol, the polymer chains produced exclusively hollow spheres of 400 nm in size. The depth profile of these objects clearly confirms their hollow structures (see inset in Figure 5h). The P-TCD-6EG polymer was also showed an excellent morphological transition from nanofibers to spherical nanoassemblies in THF + water solvent mixture (see Figure 6a−f). FE-SEM and AFM images showed that the polymer chains exhibited the helical nanofibrous morphology in THF (see Figure 6, parts a and b). Upon increasing the water amount in the solvent mixture, the polymer transformed into hollow spherical assemblies as evident from their AFM images in Figure 6c−f. At 60 and 80% THF in water, the polymer produced exclusively hollow-spheres (see Figure 6, parts c and d). At 40% THF in water (see Figure 6e) and the dialyzed aqueous solution (see Figure 6f, in water alone), the polymers were self-assembled into <200 nm tiny nanoparticles, which was confirmed by the AFM image

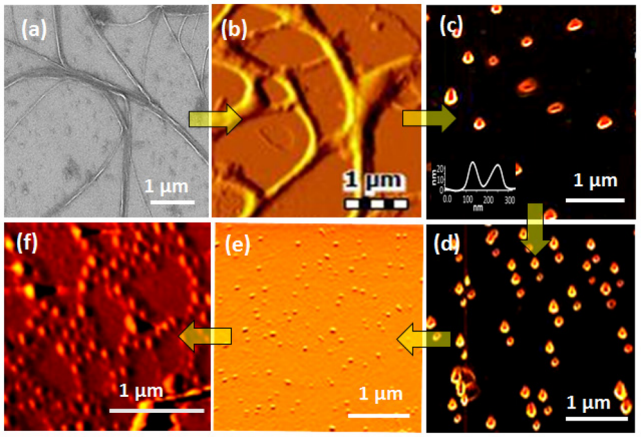

Figure 6. P-TCD-6EG polymer FE-SEM image in THF (a); AFM image in THF (b), in 20% (c), 40% (d), and 60% (e) water/THF composition, and in water (f). The concentrations of the polymers were maintained as 1×10^{-5} M.

in Figure 6f. FE-SEM and high resolution TEM (HR-TEM) images of the dialyzed nanoparticles were recorded and showed in Figure S11. These electron microscopic images exhibited the formation of spherical nanoparticles.

In order to prove that the spherical nanoassemblies were pre-existed in the polymer solution and visualized as individual objects during imaging rather than they were produced during the solvent evaporation process; the polymer solutions were subjected to dynamic light scattering analysis. DLS histograms of THF + water and chloroform + methanol mixtures are shown in Figure 7. The dialyzed aqueous solution exhibited monomodal distribution with respect to particles in the ranges of 200 ± 20 nm (see Figure 7a). DLS histograms retained its monomodal; however the size of the spherical objects became larger with a decrease in the amount of water in THF+water combinations. The size of the particles increase from 200 nm to 1.0 μm for 60% and 40% of water in THF (see Figure 7, parts b and c). This trend clearly suggests that upon increasing the THF concentration, the tightly packed nanoparticles slowly uncoiled into large size aggregates. The DLS histograms of chloroform+methanol solvent combination is also exhibited similar trend (see Figures 7d to 7f). For example, the polymers were self-assembled as monomodal aggregated species in 60%

DOI: 10.1021/acs.macromol.6b00660
Macromolecules XXXX, XXX, XXX−XXX

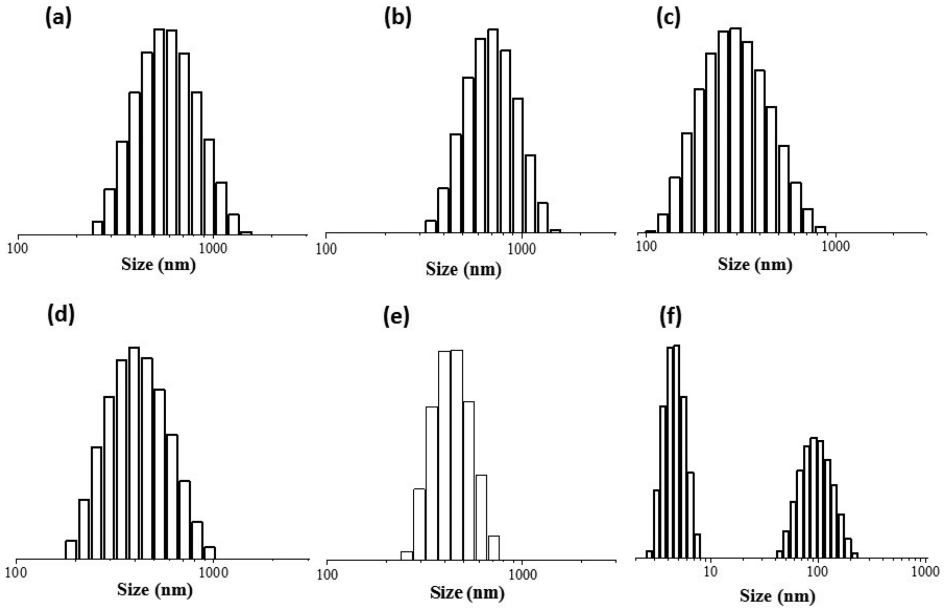

Figure 7. DLS histograms of P-TCD-6EG in water (a) and in 60% (b), and 40% (c) water/THF composition. The concentration of the polymers were maintained as 2.5×10^{-5} M (d). DLS histograms of P-TCD-6EG in 60% (d), 40%(e), and 20% (f) methanol/chloroform composition. The concentrations of the polymers were maintained as 2.5×10^{-4} M.

and 40% methanol/chloroform (see Figures 7, parts d and e), and it became multimodal with larger aggregates in 20% methanol/chloroform (see Figure 7f). These trends indicate that the polymer self-assembled as tightly packed spherical objects in bad solvents (in methanol or water) and expanded to larger sizes in good solvents (THF or chloroform) (for the DLS histograms of other good and bad solvent combination, see Figures S12 and S13). Thus, the DLS data direct evidence that the morphological transitions from spherical to nanofibrous and vice versa are indeed occurred by the ability of the polymer chains to preassemble in the solvent combinations and not occurred by the solvent evaporation process while sample preparation for imaging. The segmented polymer chains were solvated in good solvents (like chloroform and THF) in expanded chain conformation. These solvated chains undergo interchain aggregation to produce long fibril structure in the drop castes films (see Figures 5a and 6a). On the other hand, in poor solvents (like methanol and water), the polymer chains are collapsed to adapt coil-like conformation and these coiled chains would prefer to aggregate together to produce nanoparticles (see Figures 5d and 6f). Thus, polymer topology played a crucial role on the self-assembly of these custom designed segmented OPV polymers.

Based on the photophysical studies, color-tuning ability, morphological evidence, and DLS studies; the self-assembly of the segmented polymers are schematically drawn and shown in Figure 1. The following conclusion may be drawn for the unique self-assembly of custom-designed segmented TCD-OPV polymer. The polymer existed as solvated chains in good solvents (THF or chloroform) and exhibits blue-luminescence. The drop casted film from the good solvent produces helical nanofibrous morphology. Upon increasing the bad solvent composition (water or methanol) in the polymer solution (THF + water or chloroform + methanol); the polymer chains experienced strong aromatic $\pi-\pi$ stacking and produced layered intermediates via hydrophobic and hydrophilic interaction by the amphiphilic backbones. At this stage, the OPV π-core exists both in the aggregated (greenish yellow) and isolated form (blue) and their combination produced white color emission. The increase in the bad solvent amount (methanol or water) increase the packing further and the layered assembly folded as spherical hollow particles and emit greenish yellow emission. The dialyzed polymer solution (in water alone); self-assembled structure appeared as tiny nanoparticles (no hollow structures are observed in the microscopic analysis) and luminescence as bright yellow color. Hence, the present segmented polymer design is very unique in producing diverse nanoassemblies such as nanofibers and hollow spheres and further capable of exhibiting luminescence color-tuning from blue-to-white-to-yellow in a single π-conjugated system.

Cytotoxicity and Bioimaging. Water-soluble π-conjugated polymers are emerging as important classes of luminescent probes for cellular imaging in biological system.[1,2,55] The custom designed segmented TCD-OPV polymer produced very stable luminescent aqueous nanoparticles. Thus, these nanoparticles were employed as a bioimaging probe for cancer cells. The cytotoxicity of the polymer nanoparticles were investigated in cervical (HeLa) and breast cancer (MCF 7) cell lines. The cytotoxicity of the polymer was tested in these cell lines by varying their concentration up to 60 μg/mL and the data are summarized in Figure 8. The nascent polymer nanoparticles were found to be nontoxic to cells and more than 90% cell viability was

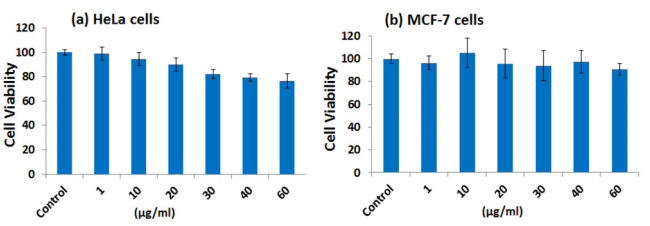

Figure 8. Cytotoxicity of P-TCD-6EG polymer nanoparticles (a) in HeLa cells and (b) in MCF-7 cells.

DOI: 10.1021/acs.macromol.6b00660
Macromolecules XXXX, XXX, XXX−XXX

observed in both cell lines. This data confirmed that the amphiphilic nanoparticles made by the segmented TCD-OPV polymers are very good biocompatible probes for cancer cells. For cellular imaging, the polymer nanoparticle was administrated to HeLa cells and their confocal images were recorded and shown in Figure 9. Since the polymer nanoparticles are

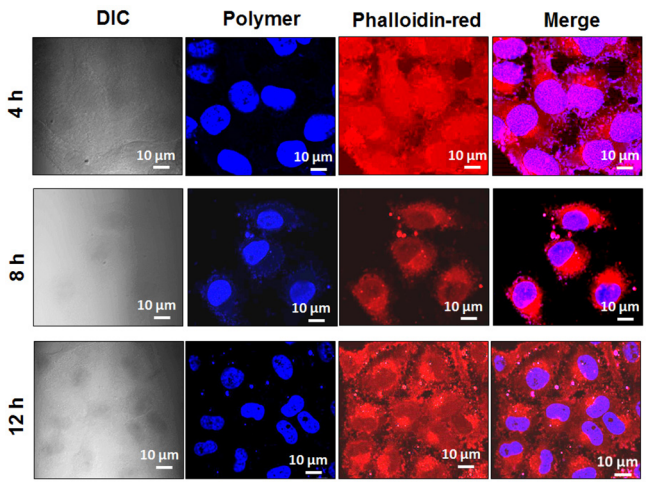

Figure 9. Confocal images of HeLa cells incubated with P-TCD-6EG polymer at 4, 8, and 12 h. The cells were observed through the blue channel to locate the polymer (OPV chromophore) fluorescence. The actin cytoskeleton network in cells was stained with phalloidin (red).

blue fluorescent, the cytoplasm of the cell was stained with Phalloidin (red fluorescent dye) and merged images distinctly showed the nucleus and cytoplasm. To study the influence of the incubation period on the polymer nanoparticles uptake; the cells were treated at various time intervals of 4, 8, and 12 h with the polymer nanoparticles. The comparison of these images revealed that the cellular uptake of the polymer nanoparticles at 4 h is almost similar to that at 8 and 12 h.

Most of the polymer nanoparticles are typically up taken by the cells through endocytosis process. Our recent studies on the polymer nanoparticles in the treatment of the breast and colon cancer cell lines supported the similar observation.[56] Typically polyaromatic drugs or nuclear staining agents bind to the DNA in the nucleus by intercalation and aromatic π-stacking interaction.[56] Thus, the newly designed OPV aromatic π-core may be underwent similar binding mechanism at the nucleus. Very recently we observed a similar trend for the binding of OPV based biodegradable block copolymer nanoassemblies.[55] These nanoparticles were found to be selectively accumulated in the nucleus of the cells. The merged image did not show any trace of the polymer particles in the cytoplasm. This observation makes these segmented OPV nanoparticles as ideal markers for the nucleus. These experiments confirmed that the blue luminescent nascent polymer nanoparticles are highly cell penetrable and very useful for cellular imaging applications in cancer diagnostics. Since OPV cores are very new entries for cellular imaging and the present manuscript explored their reproducibility in both cervical (HeLa) and breast (MCF 7) cancer cell lines; the nuclear staining of OPVs would be expected to be similar for other cells as well. Further detail studies of DNA-OPV chromophores interactions are required to confirm this hypothesis. Owing to their biocompatibility, the structure of the segmented polymer can be further improvised to them as efficient anticancer drug carries along with intrinsic fluorescence as dual function delivery-cum-biomarkers in cancer therapy. Currently, research work is focused on these directions to explore these segmented conjugated polymers in cancer therapy.

CONCLUSION

In summary, a new series of amphiphilic segmented π-conjugated polymers were designed and developed for studying their solvent-mediated diverse supramolecular assemblies and employed their aqueous nanoassemblies as a fluorescent probe for bio- imaging in cancer cells. The π-conjugated core was constituted by oligo-phenylenevinylene (OPV) units with variable anchoring units at the periphery to tune their rigidity and solubility for self-organization. The flexible segments were chosen from oligoethyleneoxy units and they were placed in the backbone of the chains to yield amphiphilic segment OPV polymers. Solvent induced aggregation ability of the segmented polymers were investigated in chloroform + methanol, THF + water, and water alone. The π-conjugated OPV core was found to undergo strong aromatic $\pi-\pi$ stacking upon increasing the composition of the bad solvent (water or methanol) in the polymer solution. Both types of the OPV cores as well as the oligoethyleneoxy chain lengths were found to play an important role in directing the segmented polymers for diverse self-assembly. The polymer P-TCD-6EG was found to produce helical nanofibrous morphology in good solvents (chloroform or THF) and it underwent a morphological transition from fibers to hollow spheres upon varying the solvent composition. This morphological transition was also accompanied by the fluorescence color tuning by the OPV core. It was found that the chromophores exhibited blue-to-white-to-yellow color change along with the morphological transitions. Dynamic light scattering studies confirmed that the segmented polymers indeed produced stable spherical nanoaggregates of 200 nm in the solution. Steady state fluorescence studies and time-resolved fluorescent decay dynamic analysis confirmed the color tunability in the segmented π-conjugated polymers. The polymers produced stable nanoparticles assemblies in water with luminescent properties. Cytotoxicity in cervical and breast cancer cells revealed that these segmented polymer nanoparticles are nontoxic to cells. Confocal microscopy imaging revealed that the polymer nanoparticles selectively accumulated in the nucleus. The present design explored new segmented π-conjugated polymers for producing stable aqueous nanoparticles which are successfully demonstrated as potential candidates for bioimaging applications. The segmented polymer design reported here not only restricted to OPV π-core, and in general it can be expanded to wide ranges of other π-conjugated systems to explore this new concept for material and biomedical applications.

ASSOCIATED CONTENT

Supporting Information

The Supporting Information is available free of charge on the ACS Publications website at DOI: 10.1021/acs.macromol.6b00660.

Synthesis of polymers, structural and molecular weights characterization, TGA and DSC plot, absorption and emission data, FE-SEM and AFM, and HR-TEM images, photophysical data, and NMR spectra of the monomers and polymers (PDF)

DOI: 10.1021/acs.macromol.6b00660
Macromolecules XXXX, XXX, XXX−XXX

AUTHOR INFORMATION

Corresponding Author

*(M.J.) E-mail: jayakannan@iiserpune.ac.in.

Notes

The authors declare no competing financial interest.

ACKNOWLEDGMENTS

The authors express thanks for a research grant from the Department of science and Technology (DST), New Delhi, India, under SERB Project SB/OC/OM-10/2014. The authors thank Bapurao Surnar and Sonashree Saxane from our group for cytotoxicity and cellular imaging data, respectively. We thank MHRD, New Delhi, India, for funding under FAST Scheme. K.N. thanks the UGC, New Delhi, India, for a research fellowship.

REFERENCES

(1) Li, K.; Liu, B. Polymer-encapsulated organic nanoparticles for fluorescence and photoacoustic imaging. *Chem. Soc. Rev.* **2014**, *43*, 6570−6597.

(2) Zhu, C.; Liu, L.; Yang, Q.; Lv, F.; Wang, S. Water-Soluble Conjugated Polymers for Imaging, Diagnosis, and Therapy. *Chem. Rev.* **2012**, *112*, 4687−4735.

(3) Bunz, U. H. F.; Seehafer, K.; Bender, M.; Porz, M. Poly(aryleneethynylene)s (PAE) as paradigmatic sensor cores. *Chem. Soc. Rev.* **2015**, *44*, 4322−4336.

(4) Thomas, S. W., III; Joly, G. D.; Swager, T. M. Chemical Sensor Based on Amplifying Fluorescent Conjugated Polymers. *Chem. Rev.* **2007**, *107*, 1339−1386.

(5) Kim, H. N.; Ren, W. X.; Kim, J. S.; Yoon, J. Fluorescent and colorimetric sensors for detection of lead, cadmium, and mercury ions. *Chem. Soc. Rev.* **2012**, *41*, 3210−3244.

(6) Wu, Y.; Tan, Y.; Wu, J.; Chen, S.; Chen, Y. Z.; Zhou, X.; Jiang, Y.; Tan, C. Fluorescence Array-Based Sensing of Metal Ions Using Conjugated Polyelectrolytes. *ACS Appl. Mater. Interfaces* **2015**, *7*, 6882−6888.

(7) McQuade, D. T.; Pullen, A. E.; Swager, T. M. Conjugated Polymer-Based Chemical Sensors. *Chem. Rev.* **2000**, *100*, 2537−2574.

(8) Bunz, U. H. F. Poly(aryleneethynylene)s: Syntheses, Properties, Structures, and Applications. *Chem. Rev.* **2000**, *100*, 1605−1644.

(9) Xu, X.; Liu, R.; Li, L. Nanoparticles made of π-conjugated compounds targeted for chemical and biological applications. *Chem. Commun.* **2015**, *51*, 16733−16749.

(10) Ding, D.; Li, K.; Zhu, Z.; Pu, K.; Hu, Y.; Jiang, X.; Liu, B. Conjugated polyelectrolyte−cisplatin complex nanoparticles for simultaneous in vivo imaging and drug tracking. *Nanoscale* **2011**, *3*, 1997−2002.

(11) Feng, L.; Liu, L.; Lv, F.; Bazan, G. C.; Wang, S. Preparation and Biofunctionalization of Multicolor Conjugated Polymer Nanoparticles for Imaging and Detection of Tumor Cells. *Adv. Mater.* **2014**, *26*, 3926−3930.

(12) Feng, X.; Tang, Y.; Duan, X.; Liu, L.; Wang, S. Lipid-modified conjugated polymer nanoparticles for cell imaging and transfection. *J. Mater. Chem.* **2010**, *20*, 1312−1316.

(13) Akcelrud, L. Electroluminescent polymers. *Prog. Polym. Sci.* **2003**, *28*, 875.

(14) Kilbinger, A. F. M.; Schenning, A. P. H. J.; Goldoni, F.; Feast, W. J.; Meijer, E. W. Chiral Aggregates of α,ω-Disubstituted Sexithiophenes in Protic and Aqueous Media. *J. Am. Chem. Soc.* **2000**, *122*, 1820−1821.

(15) Jiang, L.; Hughes, R. C.; Sasaki, D. Y. Supramolecular assembly of a quaterthiophene surfactant. *Chem. Commun.* **2004**, 1028−1029.

(16) Henze, O.; Feast, W. J.; Gardebien, F.; Jonkheijm, P.; Lazzaroni, R.; Leclere, P.; Meijer, E. W.; Schenning, A. P. H. J. Chiral Amphiphilic Self-Assembled α,α'-Linked Quinque-, Sexi-, and Septithiophenes: Synthesis, Stability and Odd−Even Effects. *J. Am. Chem. Soc.* **2006**, *128*, 5923.

(17) Schenning, A. P. H. J.; Kilbinger, A. F. M.; Biscarini, F.; Cavallini, M.; Cooper, H. J.; Derrick, P. J.; Feast, W. J.; Lazzaroni, R.; Leclere, P.; McDonell, L. A.; Meijer, E. W.; Meskers, S. C. J. Supramolecular Organization of α,α'-Disubstituted Sexithiophenes. *J. Am. Chem. Soc.* **2002**, *124*, 1269.

(18) Abbel, R.; van der Weegen, R.; Meijer, E. W.; Schenning, A. P. H. J. Multicolour self-assembled particles of fluorene-based bolaamphiphiles. *Chem. Commun.* **2009**, 1697.

(19) Shin, S.; Lim, S.; Kim, Y.; Kim, T.; Choi, T.; Lee, M. Supramolecular Switching between Flat Sheets and Helical Tubules Triggered by Coordination Interaction. *J. Am. Chem. Soc.* **2013**, *135*, 2156−2159.

(20) Lee, E.; Jeong, Y.; Kim, J.; Lee, M. Controlled Self-Assembly of Asymmetric Dumbbell-Shaped Rod Amphiphiles: Transition from Toroids to Planar Nets. *Macromolecules* **2007**, *40*, 8355−8360.

(21) Ryu, J.; Lee, M. Transformation of Isotropic Fluid to Nematic Gel Triggered by Dynamic Bridging of Supramolecular Nanocylinders. *J. Am. Chem. Soc.* **2005**, *127*, 14170−14171.

(22) Moon, K.; Kim, H.; Lee, E.; Lee, M. Self-Assembly of T-Shaped Aromatic Amphiphiles into Stimulus-Responsive Nanofibers. *Angew. Chem., Int. Ed.* **2007**, *46*, 6807.

(23) Moon, K.; Lee, E.; Lee, M. Synthesis and self-assembly of propeller-shaped amphiphilic molecules. *Chem. Commun.* **2008**, 3061−3063.

(24) Rest, C.; Mayoral, M. J.; Fucke, K.; Schellheimer, J.; Stepanenko, V.; Fernàndez, G. Self-Assembly and (Hydro)gelation Triggered by Cooperative $\pi-\pi$ and Unconventional C[BOND]H···X Hydrogen Bonding Interactions. *Angew. Chem., Int. Ed.* **2014**, *53*, 700−705.

(25) Ajayaghosh, A.; Varghese, R.; Mahesh, S.; Praveen, V. K. From Vesicles to Helical Nanotubes: A Sergeant-and-Soldiers Effect in the Self-Assembly of Oligo(p-phenyleneethynylene)s. *Angew. Chem., Int. Ed.* **2006**, *45*, 7729.

(26) Shin, S.; Gihm, S. H.; Park, C. R.; Kim, S.; Park, S. Y. Water-Soluble Fluorinated and PEGylated Cyanostilbene Derivative: An Amphiphilic Building Block Forming Self-Assembled Organic Nanorods with Enhanced Fluorescence Emission. *Chem. Mater.* **2013**, *25*, 3288−3295.

(27) Hulvat, J. F.; Sofos, M.; Tajima, K.; Stupp, S. I. Self-Assembly and Luminescence of Oligo(p-phenylene vinylene) Amphiphiles. *J. Am. Chem. Soc.* **2005**, *127*, 366−372.

(28) Zhang, X.; Gorl, D.; Wurthner, F. White-light emitting dye micelles in aqueous solution. *Chem. Commun.* **2013**, *49*, 8178−8180.

(29) Zhang, X.; Chen, Z.; Wurthner, F. Morphology control of fluorescent nanoaggregates by co-self-assembly of wedge- and dumbbell-shaped amphiphilic perylene bisimides. *J. Am. Chem. Soc.* **2007**, *129*, 4886−4887.

(30) Kim, Y.; Li, W.; Shin, S.; Lee, M. Development of Toroidal Nanostructures by Self-Assembly: Rational Designs and Applications. *Acc. Chem. Res.* **2013**, *46*, 2888−2897.

(31) Molla, M. R.; Ghosh, S. Aqueous self-assembly of chromophore-conjugated amphiphiles. *Phys. Chem. Chem. Phys.* **2014**, *16*, 26672−26683.

(32) Wang, H.; Wang, H. H.; Urban, V. S.; Littrell, K. C.; Thiyagarajan, P.; Yu, L. Syntheses of Amphiphilic Diblock Copolymers Containing a Conjugated Block and Their Self-Assembling Properties. *J. Am. Chem. Soc.* **2000**, *122*, 6855−6861.

(33) Luo, Y.; Liu, H.; Xi, F.; Li, L.; Jin, X.; Han, C. C.; Chan, C. Supramolecular Assembly of Poly(phenylene vinylene) with Crown Ether Substituents To Form Nanoribbons. *J. Am. Chem. Soc.* **2003**, *125*, 6447−6451.

(34) Lee, E.; Hammer, B.; Kim, J. K.; Page, Z.; Emrick, T.; Hayward, R. C. Hierarchical Helical Assembly of Conjugated Poly(3-hexylthiophene)-block-poly(3-triethylene glycol thiophene) Diblock Copolymers. *J. Am. Chem. Soc.* **2011**, *133*, 10390−10393.

(35) Hu, Y.; Su, M.; Ma, C.; Yu, Z.; Liu, N.; Yin, J.; Ding, Y.; Wu, Z. Multiple Stimuli-Responsive and White-Light Emission of One-Pot Synthesized Block Copolymers Containing Poly(3-hexylthiophene) and Poly(triethyl glycol allene) Segments. *Macromolecules* **2015**, *48*, 5204−5212.

DOI: 10.1021/acs.macromol.6b00660
Macromolecules XXXX, XXX, XXX−XXX

(36) Yang, Z.; Sokolik, I.; Karasz, F. E. A Soluble Blue-Light-Emitting Polymer. *Macromolecules* **1993**, *26*, 1188−1190.
(37) Chen, Y.; Xu, Y.; Perry, K.; Sokolov, A. P.; More, K.; Pang, Y. Achieving Diameter-Selective Separation of Single-Walled Carbon Nanotubes by Using Polymer Conformation-Confined Helical Cavity. *ACS Macro Lett.* **2012**, *1*, 701−705.
(38) Chen, Y.; Malkovskiy, A.; Wang, X.-Q.; Lebron-Colon, M.; Sokolov, A. P.; Perry, K.; More, K.; Pang, Y. Selection of Single-Walled Carbon Nanotube with Narrow Diameter Distribution by Using a PPE−PPV Copolymer. *ACS Macro Lett.* **2012**, *1*, 246−251.
(39) Lokey, R. S.; Iverson, B. L. Synthetic molecules that fold into a pleated secondary structure in solution. *Nature* **1995**, *375*, 303−305.
(40) Gabriel, G. J.; Sorey, S.; Iverson, B. L. Altering the Folding Patterns of Naphthyl Trimers. *J. Am. Chem. Soc.* **2005**, *127*, 2637−2640.
(41) Ghosh, S.; Ramakrishnan, S. Structural Fine-Tuning of $(Donor−spacer−acceptor−spacer)_n$ Type Foldamers. Effect of Spacer Segment Length, Temperature, and Metal-Ion Complexation on the Folding Process. *Macromolecules* **2005**, *38*, 676−686.
(42) Ghosh, S.; Ramakrishnan, S. Aromatic donor-acceptor charge-transfer and metal-ion-complexation-assisted folding of a synthetic polymer. *Angew. Chem., Int. Ed.* **2004**, *43*, 3264−3268.
(43) Ghosh, S.; Ramakrishnan, S. Small molecule induced folding of a synthetic polymer. *Angew. Chem., Int. Ed.* **2005**, *44*, 5441−5447.
(44) Tan, T. A. T.; Clarke, T. M.; James, D.; Durrant, J. R.; White, J. M.; Ghiggino, K. P. Synthesis and photo-induced charge separation of confined conjugation length phenylene vinylene-based polymers. *Polym. Chem.* **2013**, *4*, 5305−5309.
(45) Balamurugan, A.; Reddy, M. L. P.; Jayakannan, M. π-conjugated Polymer-Eu3+ Complexes: A Versatile Luminescent Molecular probe for Temperature Sensing. *J. Mater. Chem. A* **2013**, *1*, 2256−2266.
(46) Balamurugan, A.; Kumar, V.; Jayakannan, M. Triple action Polymer Probe: Carboxylic Distilbene Fluorescent Polymer Chemosensor for Temperature, Metal-ion and Biomolecules. *Chem. Commun.* **2014**, *50*, 842−845.
(47) Goel, M.; Narasimha, K.; Jayakannan, M. Helical Self-assemblies of Segmented Poly(phenylenevinylene)s and their Hierarchical Donor-Acceptor Complexes. *Macromolecules* **2014**, *47*, 2592−2603.
(48) Narasimha, K.; Jayakannan, M. π-Conjugated Polymer Anisotroipic Organogel Nano-fibrous Assemblies for Thermo-responsive Photonic Switches. *ACS Appl. Mater. Interfaces* **2014**, *6*, 19385−19396.
(49) Goel, M.; Narasimha, K.; Jayakannan, M. Direct Evidence for Secondary Interactions in Planar and Nonplanar Aromatic π-Conjugates and Their Photophysical Characteristics in Solid-State Assemblies. *J. Phys. Chem. B* **2015**, *119*, 5102−5112.
(50) Goel, M.; Jayakannan, M. Herringbone and Helical Self-assembly of π -conjugated Molecules in Solid State through CH/π Hydrogen Bond. *Chem. - Eur. J.* **2012**, *18*, 11987−11993.
(51) Amrutha, S. R.; Jayakannan, M. Probing the π -stack Induced Molecular Aggregation in π -Conjugated Polymers, Oligomers and Their Blends of Poly(phenylenevinylene)s. *J. Phys. Chem. B* **2008**, *112*, 1119−1129.
(52) Resta, C.; Di Pietro, S. D.; Majerić Elenkov, M.; Hamersak, Z.; Pescitelli, G.; Di Bari, L. D. Consequences of Chirality on the Aggregation Behavior of Poly[2-methoxy-5-(2′-ethylhexyloxy)-p-phenylenevinylene] (MEH-PPV). *Macromolecules* **2014**, *47*, 4847−4850.
(53) Sonawane, S. L.; Asha, S. K. Blue, Green, and Orange-Red Emission from Polystyrene Microbeads for Solid-State White-Light and Multicolor Emission. *J. Phys. Chem. B* **2014**, *118*, 9467−9475.
(54) Balamurugan, A.; Reddy, M. L. P.; Jayakannan, M. Single polymer Photosensitizer for Tb3+ and Eu3+ ions: A Novel Approach for White Light Emission based on Carboxylic Functionalized poly(m-phenylenevinylene)s. *J. Phys. Chem. B* **2009**, *113*, 14128−14138.
(55) Kulkarni, B.; Surnar, B.; Jayakannan, M. Dual Functional Nanocarrier for Cellular Imaging and Drug Delivery in Cancer Cells Based on π -Conjugated Core and Biodegradable Polymer Arms. *Biomacromolecules* **2016**, *17*, 1004−1016.
(56) Pramod, P. S.; Shah, R.; Chaphekar, S.; Balasubramanian, N.; Jayakannan, M. Polysaccharide Nano-vesicular Multidrug Carrier for Synergistic Killing of Cancer Cells. *Nanoscale* **2014**, *6*, 11841−11855.

DOI: 10.1021/acs.macromol.6b00660
Macromolecules XXXX, XXX, XXX−XXX